Supporting information

Ultrafine Co-doped RuO_2 nanoparticles loaded on N-TiO_2 as a bifunctional electrocatalyst with wide pH adaptability

Yu-Jie Lu, Kai-Cheng Liu, Peng-Cheng Ji, Hai-Lang Jia*

School of Chemistry and Chemical Engineering, Jiangsu Key Laboratory of Clean Energy Storage and Conversion, Jiangsu University of Technology, Changzhou 213001, P. R. China.

Chemicals

Tetrabutyl titanate, urea, $CoCl_2 \cdot 6H_2O$ and $RuCl_3 \cdot H_2O$ were purchased from J&K CHEMICA Co., Ltd. Commercial RuO_2 and commercial Pt/C catalyst were purchased from Shanghai Macklin Biochemical Co., Ltd. Deionized water was self-made in the laboratory.

Materials characterization

The material morphology was examined using Field Emission Scanning Electron Microscope (Sigma 500) with an accelerating voltage of 30 kV and a transmission electron microscope (TEM) (JEM-2100, JEOL, Japan) operating at 200 kV. X-ray diffraction patterns (XRD) were acquired on a PANalytical X'Pert Powder diffractometer with Cu-Kα radiation. The X-ray photoelectron spectroscopy (XPS) with an Al-Kα X-ray source (Themo Escalab 250Xi) was performed to determine the surface composition. The content of Ru was determined by inductively coupled plasma optical emission spectrometry (Agilent, ICP-OES 720).

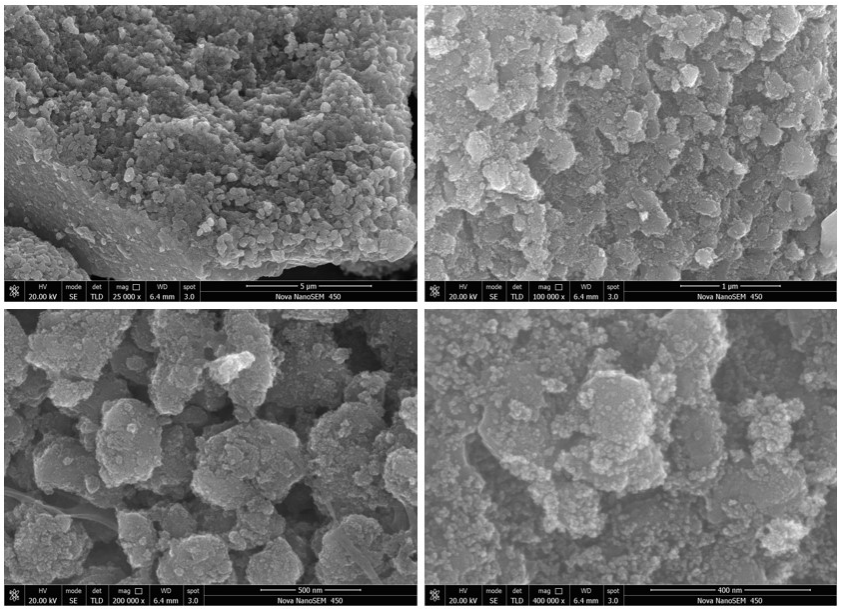

Fig. S1 SEM images of Co-RuO_2/N-TiO_2

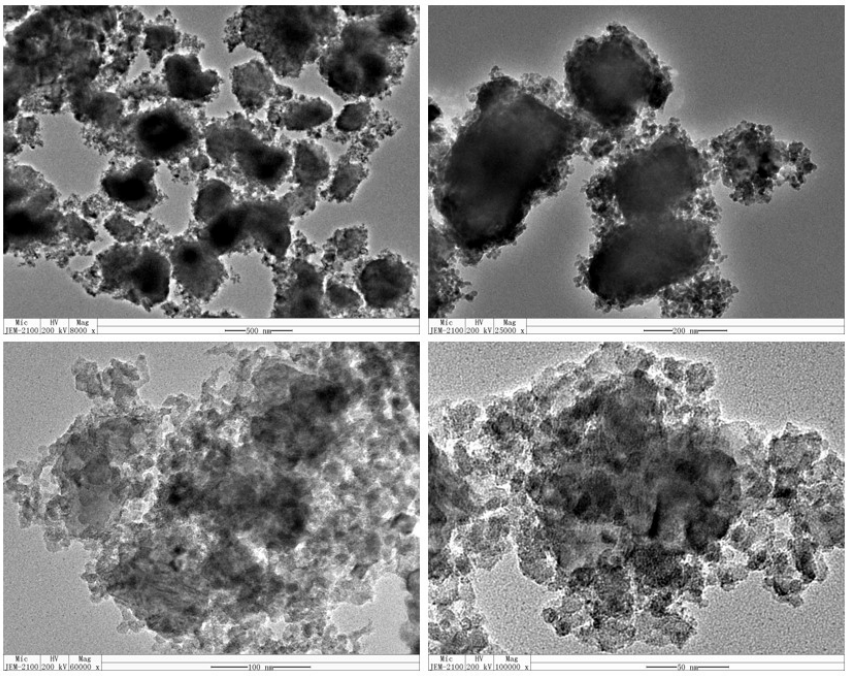

Fig. S2 TEM images of RuO_2/N-TiO_2

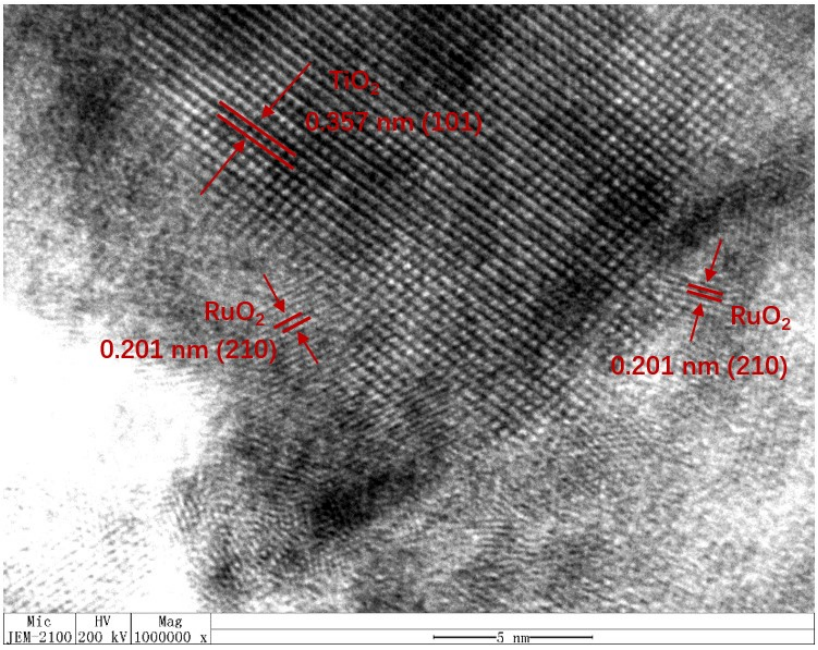

Fig. S3 HR-TEM image of RuO_2/N-TiO_2

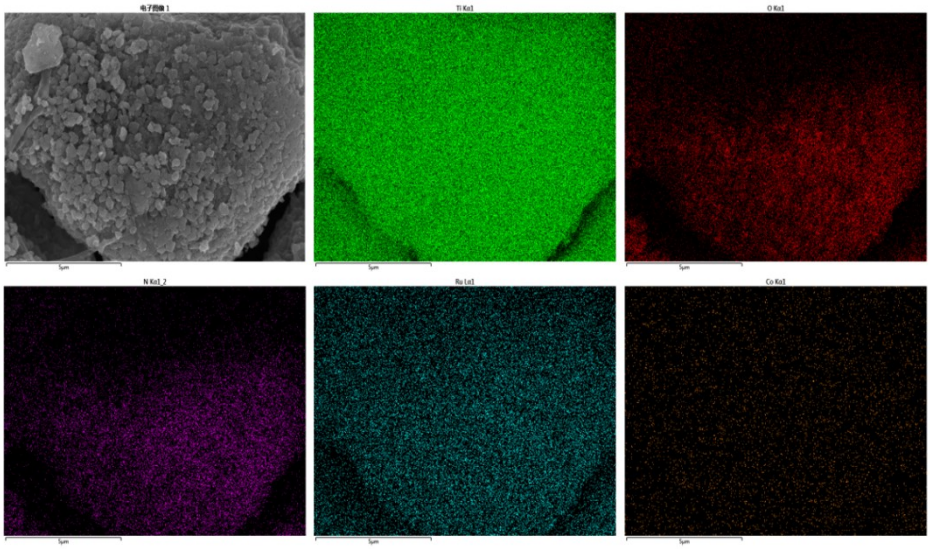

Fig. S4 EDS-mapping images of Co-RuO_2/N-TiO_2

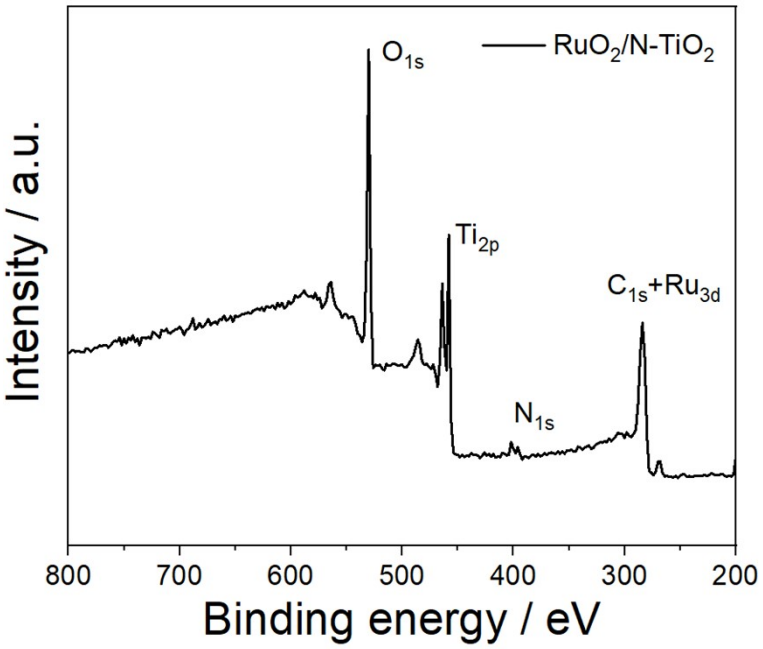

Fig. S5 XPS of RuO_2/N-TiO_2

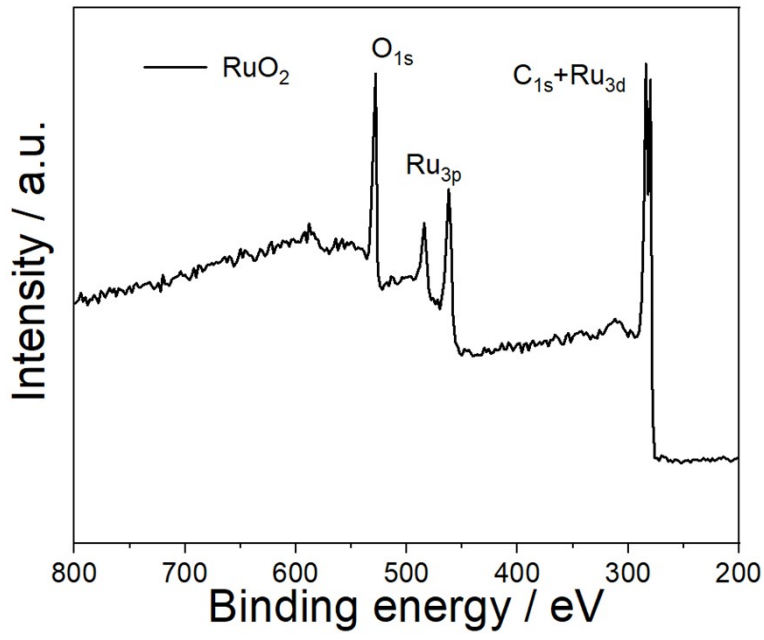

Fig. S6 XPS of RuO_2

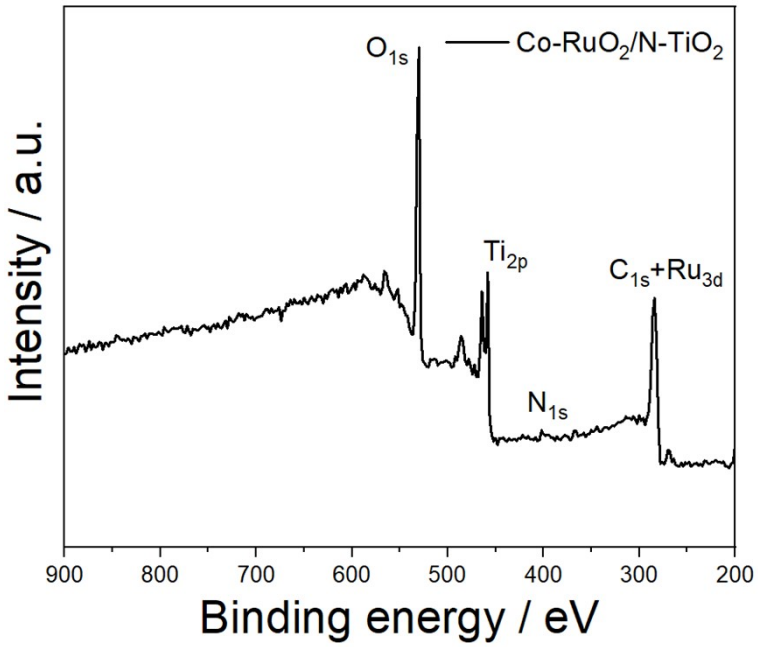

Fig. S7 XPS of Co-RuO_2/N-TiO_2

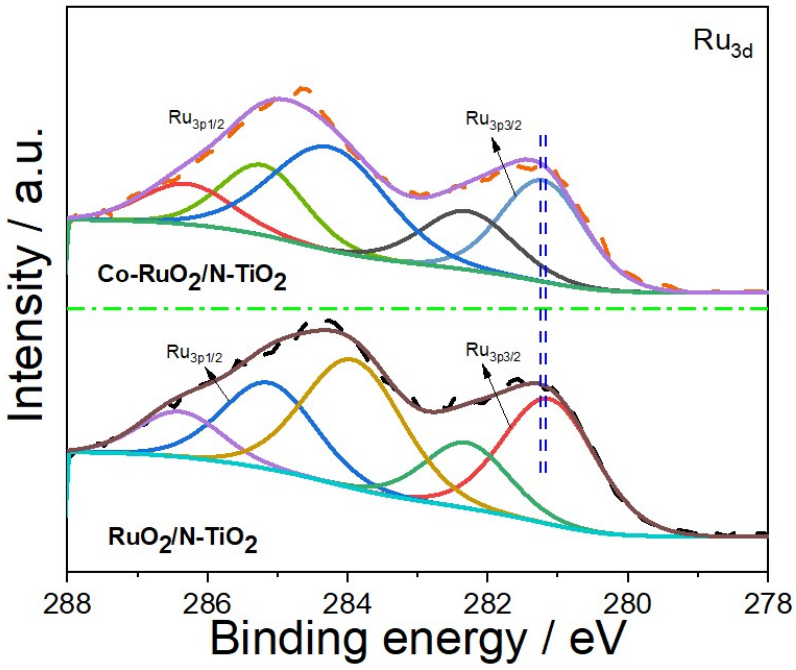

Fig. S8 High-resolution XPS spectra of Ru3d of Co-RuO_2/N-TiO_2 and RuO_2/N-TiO_2

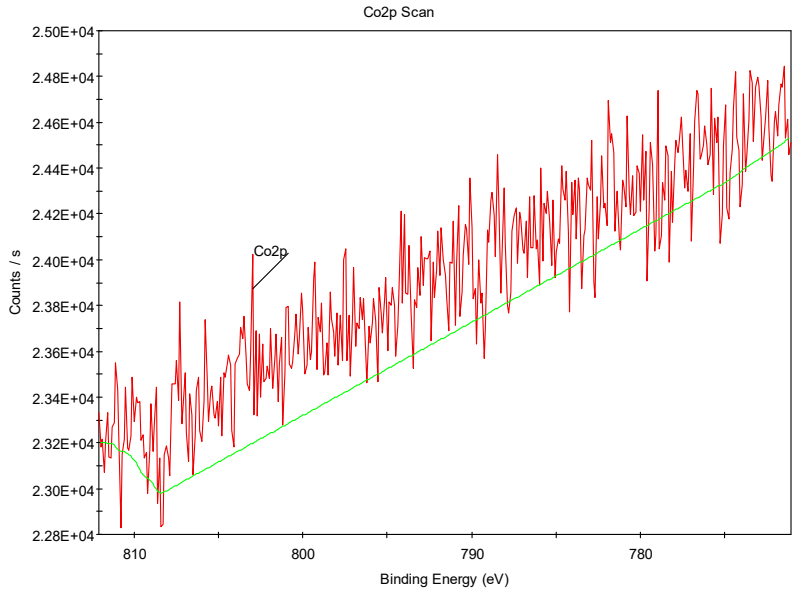

Fig. S9 High-resolution XPS spectra of Co2p of Co/N-TiO_2.

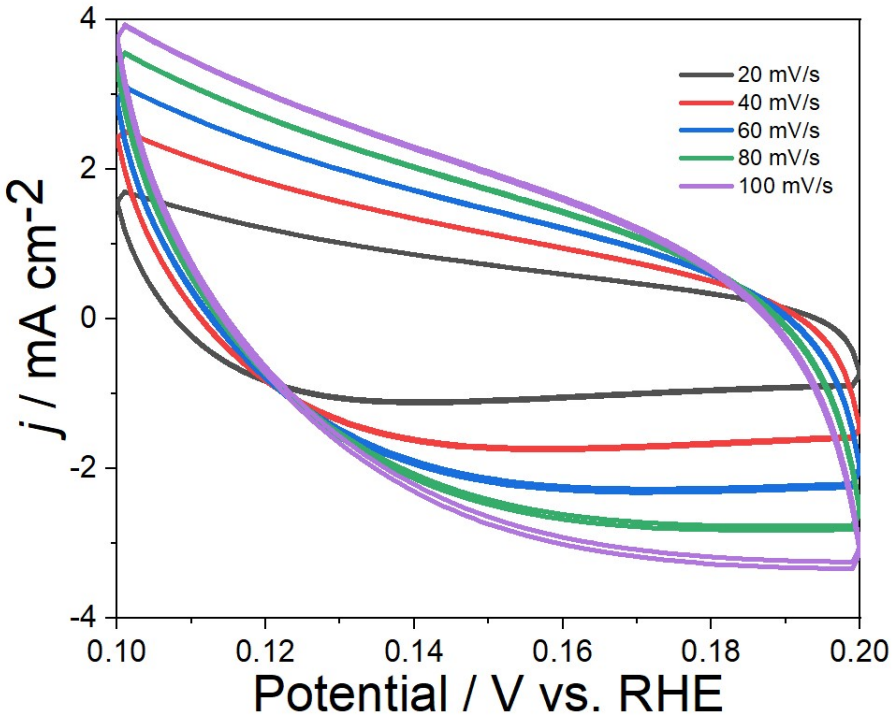

Fig. S10 CV curves of Co-RuO_2/N-TiO_2 in 1 M KOH for HER.

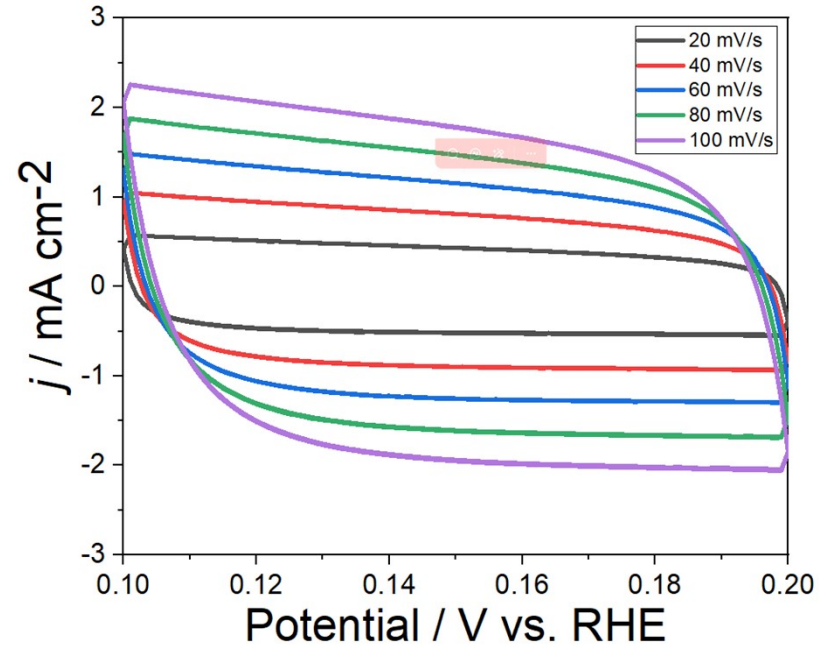

Fig. S11 CV curves of RuO_2/N-TiO_2 in 1 M KOH for HER.

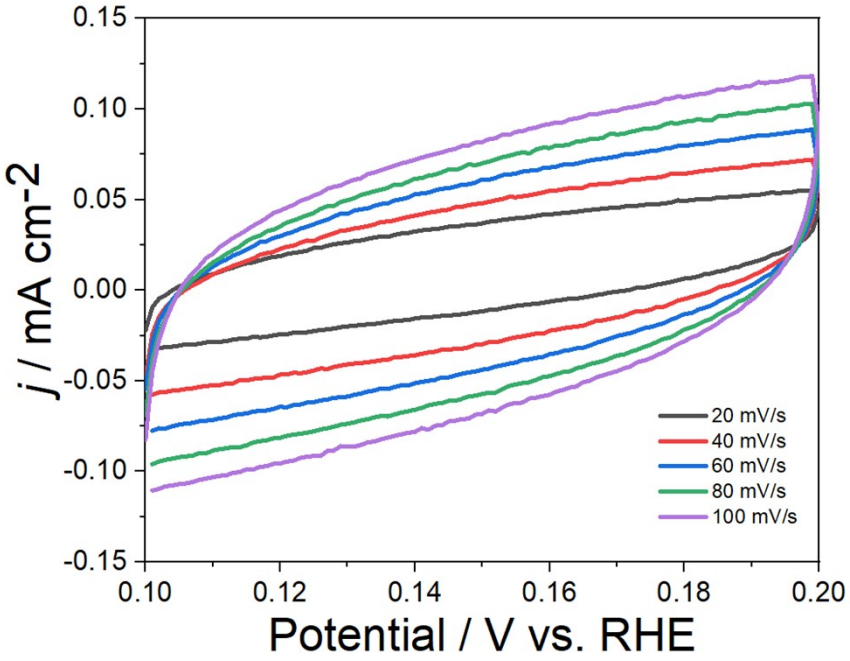

Fig. S12 CV curves of Co/N-TiO_2 in 1 M KOH for HER.

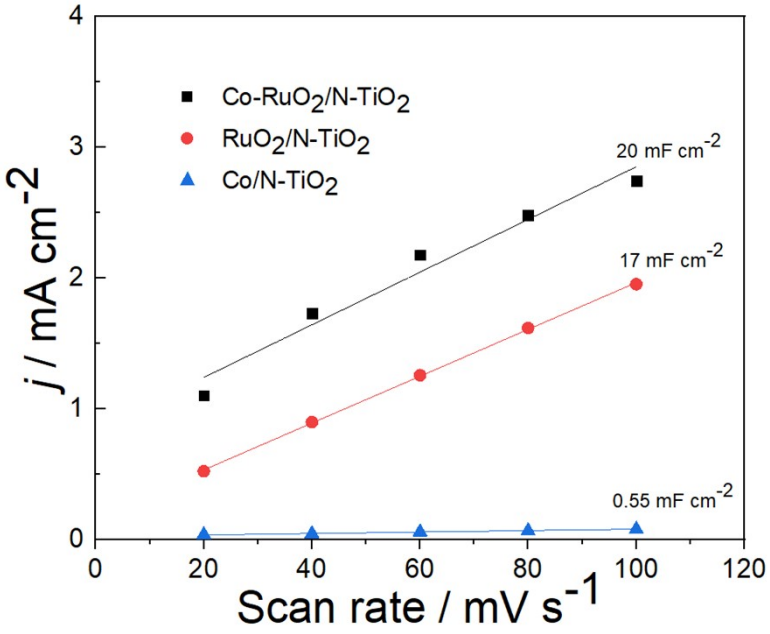

Fig. S13 The linear slope of Co-RuO_2/N-TiO_2, RuO_2/N-TiO_2 and Co/N-Ti O_2, equivalent to the double-layer capacitance (C_{dl}).

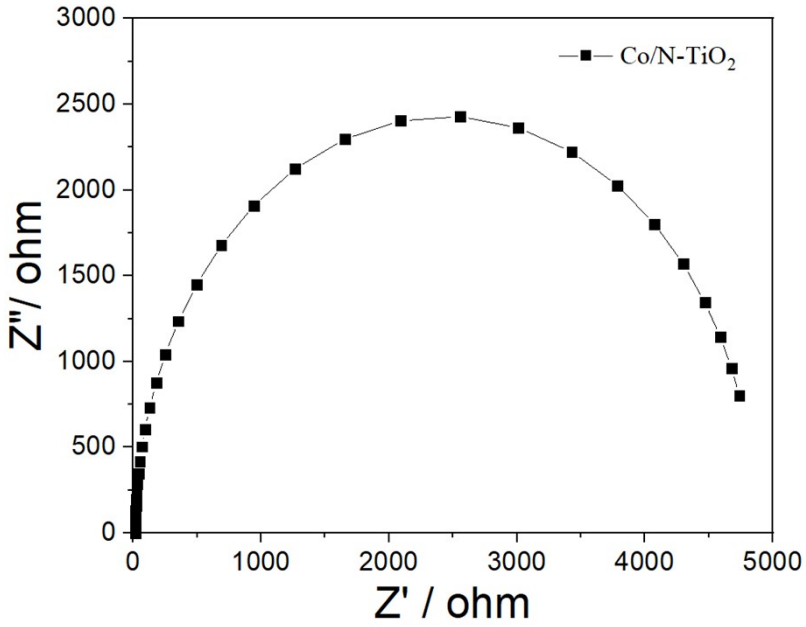

Fig. S14 EIS curve of Co/N-TiO_2 in 1 M KOH for HER.

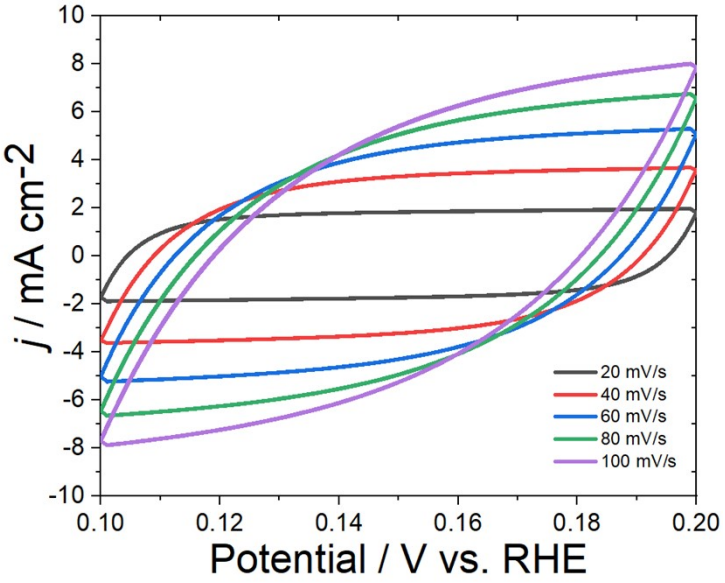

Fig. S15 CV curves of Co-RuO_2/N-TiO_2 in 0.5 M H_2SO_4 for HER.

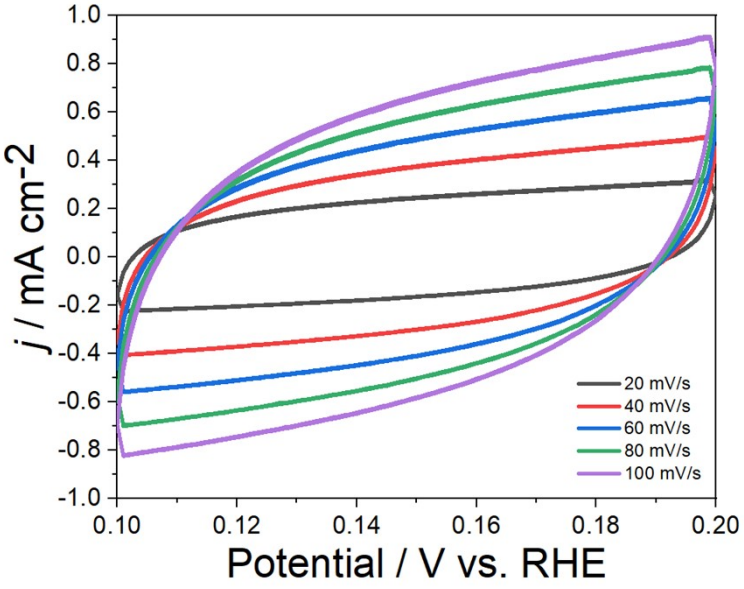

Fig. S16 CV curves of RuO_2/N-TiO_2 in 0.5 M H_2SO_4 for HER.

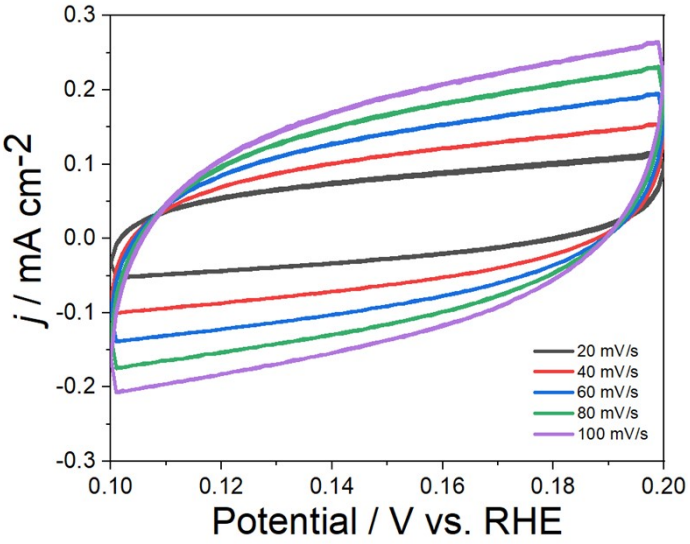

Fig. S17 CV curves of Co/N-TiO_2 in 0.5 M H_2SO_4 for HER.

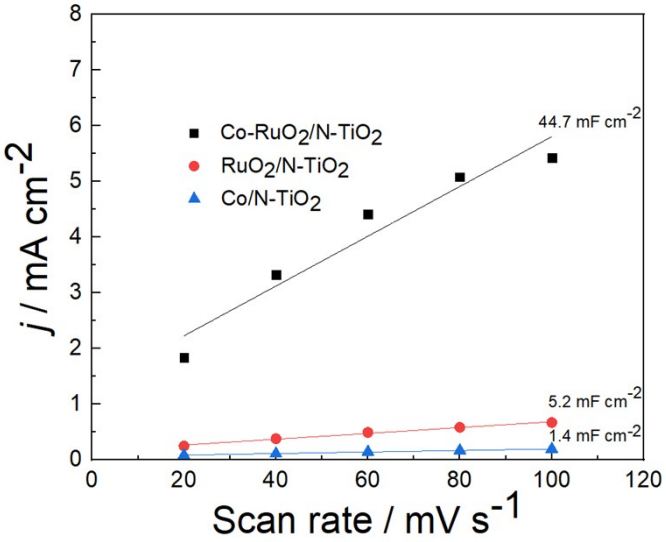

Fig. S18 The linear slope of Co-RuO_2/N-TiO_2, RuO_2/N-TiO_2 and Co/N-TiO_2, equivalent to the double-layer capacitance (C_{dl}).

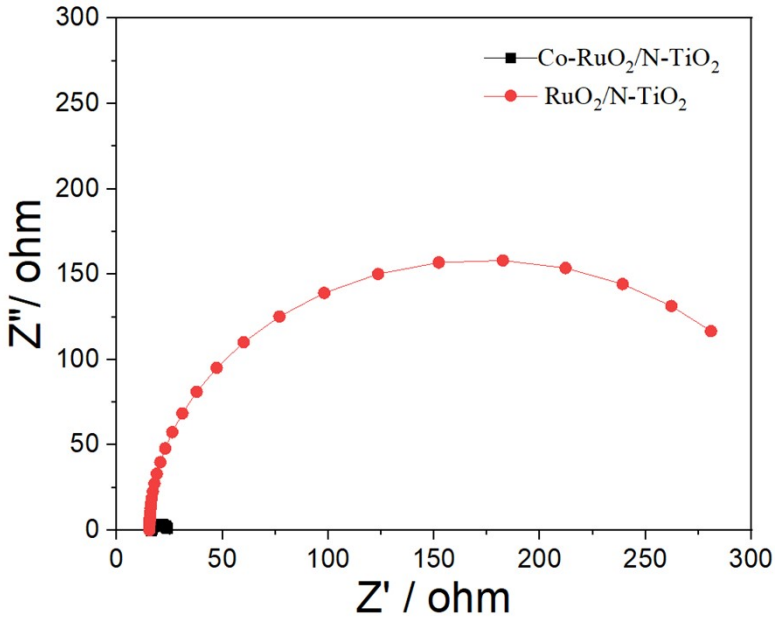

Fig. S19 EIS of Co-RuO_2/N-TiO_2 and RuO_2/N-TiO_2 in 0.5 M H_2SO_4.

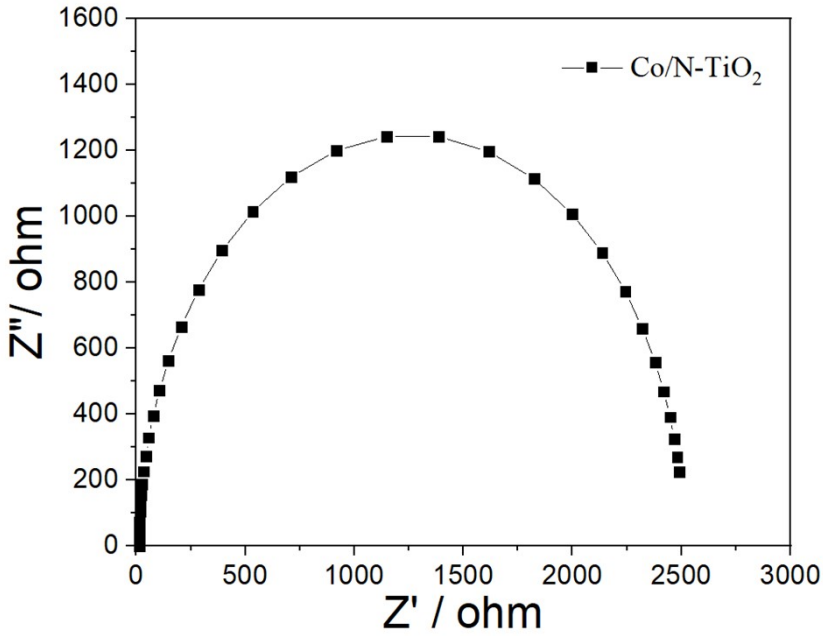

Fig. S20 EIS of Co/N-TiO_2 in 0.5 M H_2SO_4.

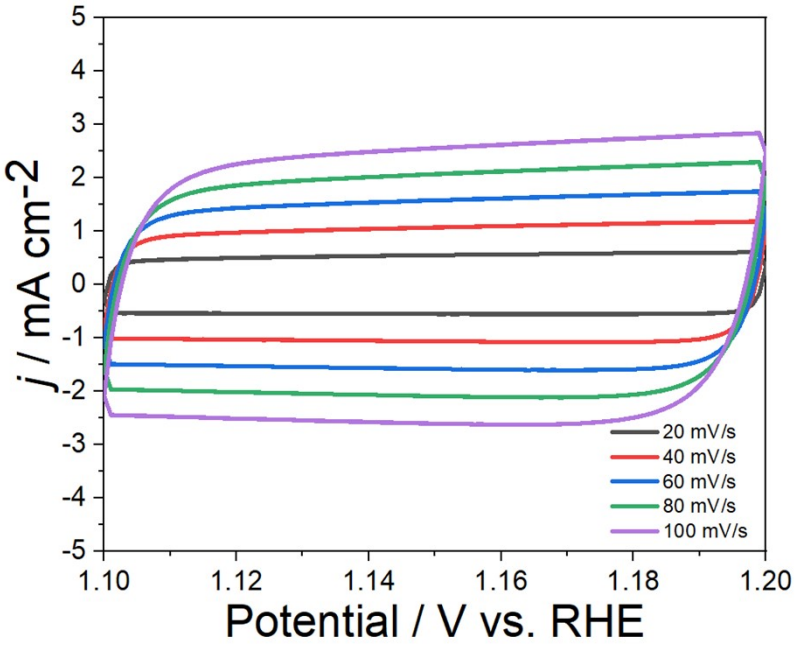

Fig. S21 CV curves of Co-RuO_2/N-TiO_2 in 0.5 M H_2SO_4 for OER.

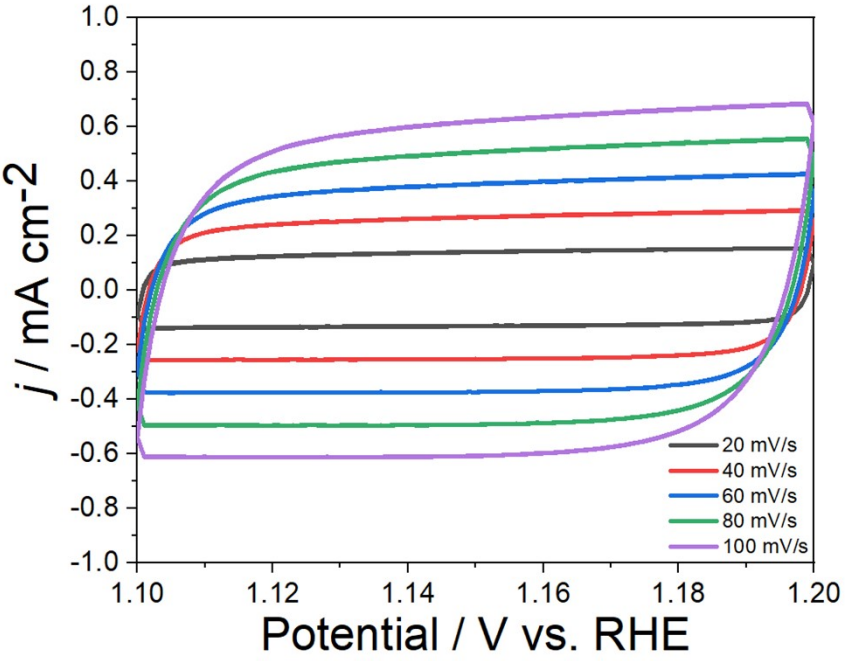

Fig. S22 CV curves of RuO_2/N-TiO_2 in 0.5 M H_2SO_4 for OER.

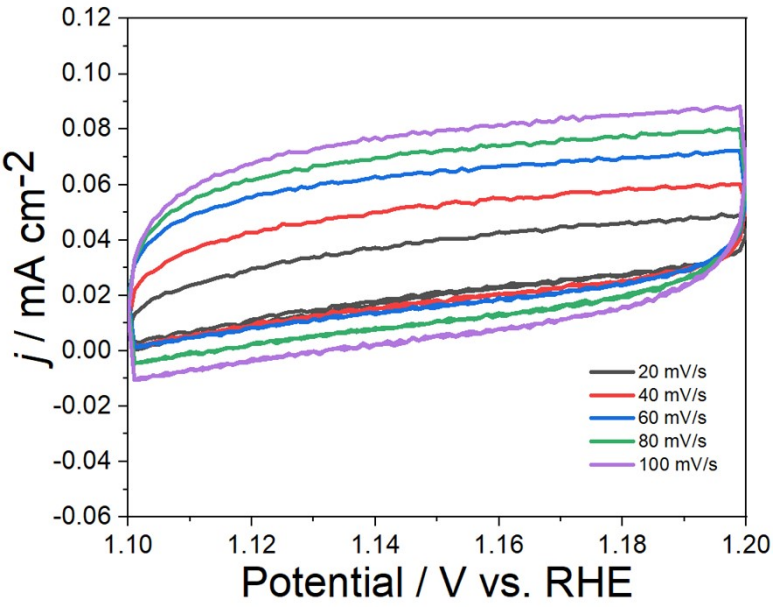

Fig. S23 CV curves of Co/N-TiO_2 in 0.5 M H_2SO_4 for OER.

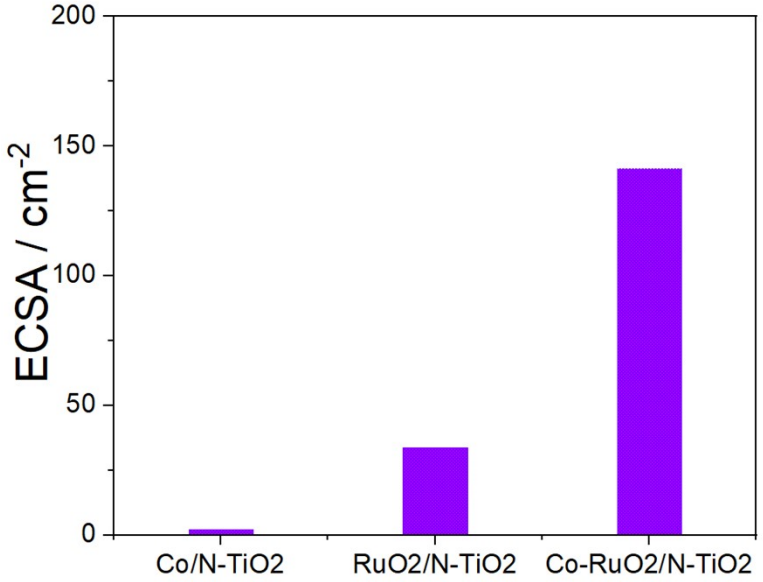

Fig. S24 ECSA of Co-RuO_2/N-TiO_2, RuO_2/N-TiO_2 and Co/N-TiO_2 in 0.5 M H_2SO_4 for OER.

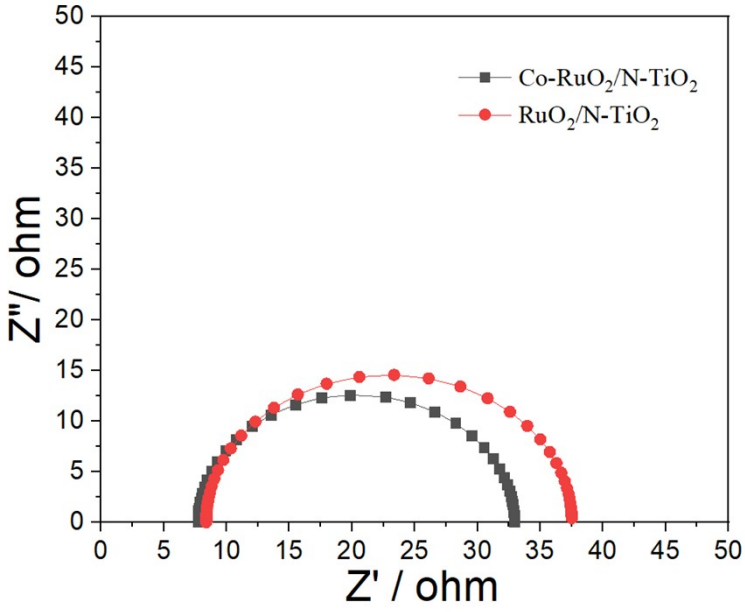

Fig. S25 EIS of Co-RuO_2/N-TiO_2 and RuO_2/N-TiO_2 in 0.5 M H_2SO_4.

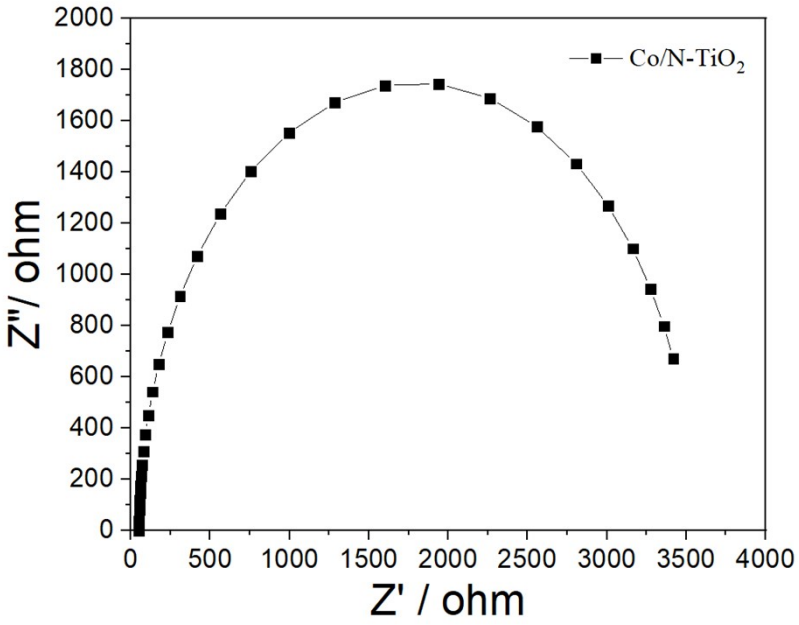

Fig. S26 EIS of Co /N-TiO_2 in 1 M KOH.

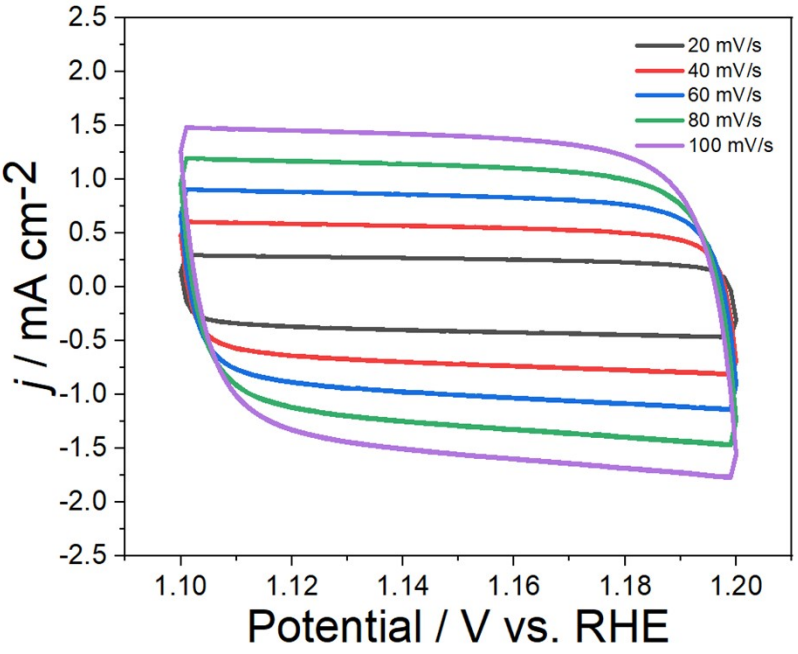

Fig. S27 CV curves of Co-RuO_2/N-TiO_2 in 1 M KOH for OER.

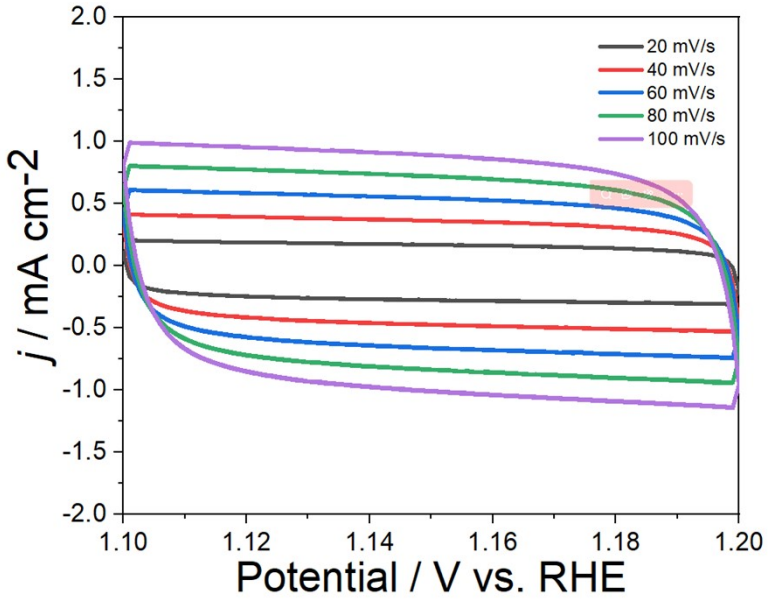

Fig. S28 CV curves of RuO_2/N-TiO_2 in 1 M KOH for OER.

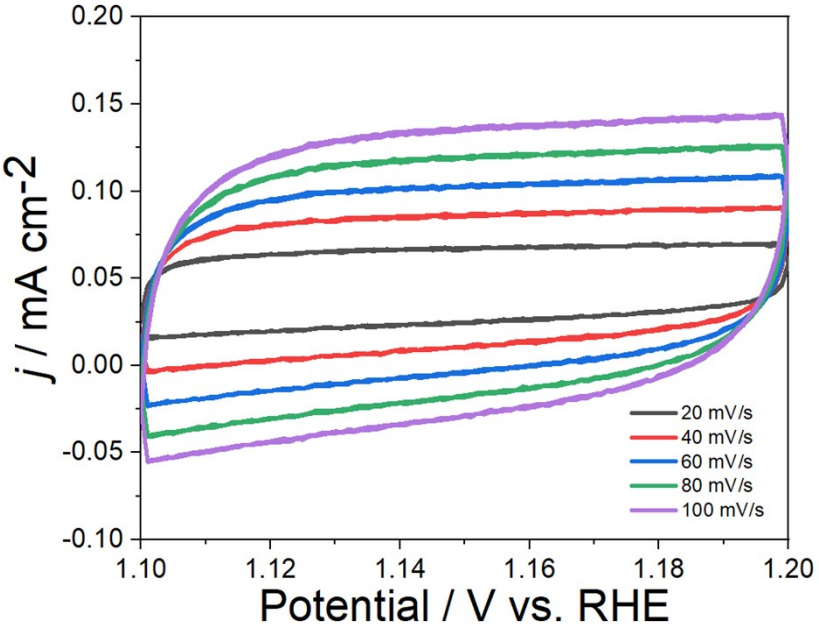

Fig. S29 CV curves of Co/N-TiO_2 in 1 M KOH for OER.

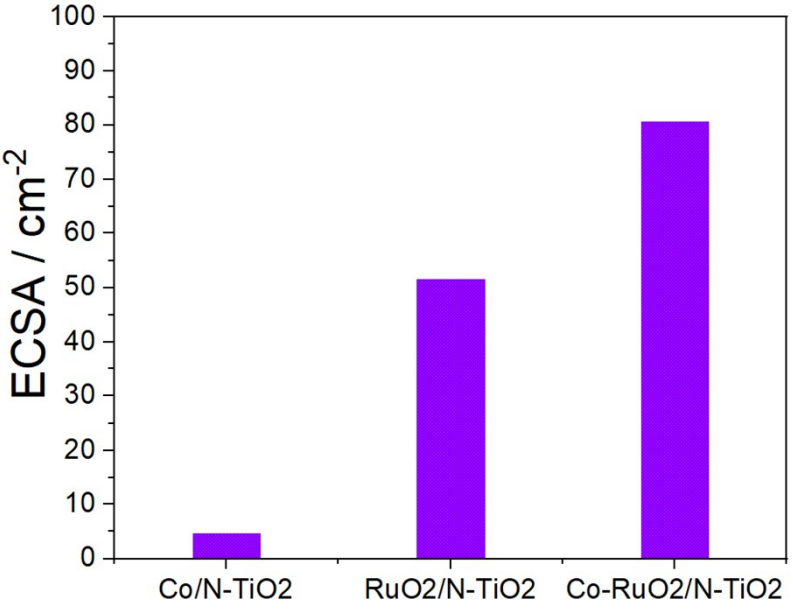

Fig. S30 ECSA of Co-RuO_2/N-TiO_2, RuO_2/N-TiO_2 and Co/N-TiO_2 in 1 M KOH for OER.

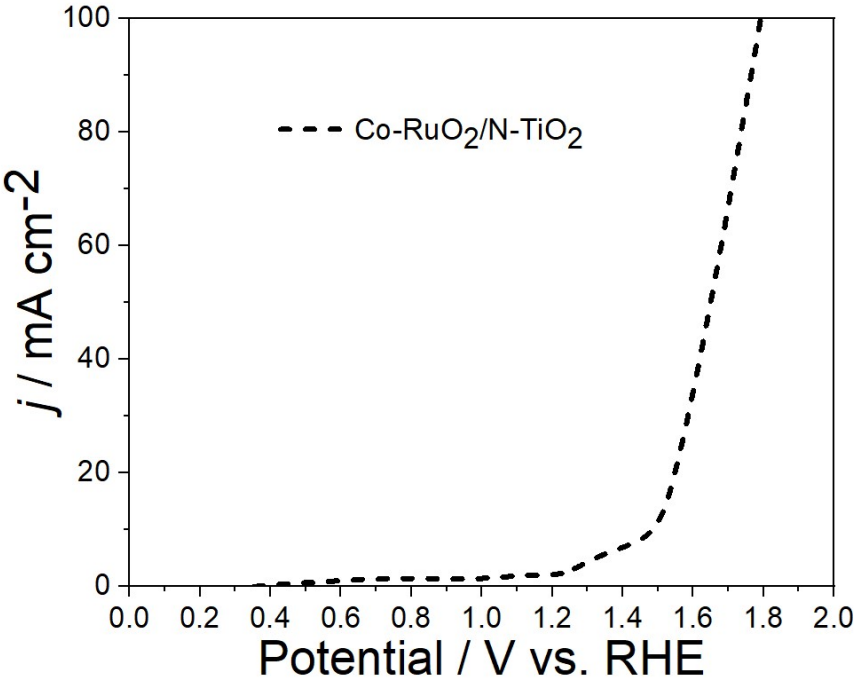

Fig. S31 Co-RuO_2/N-TiO_2 as bifunctional electrocatalyst for overall water-splitting in 1 M KOH.

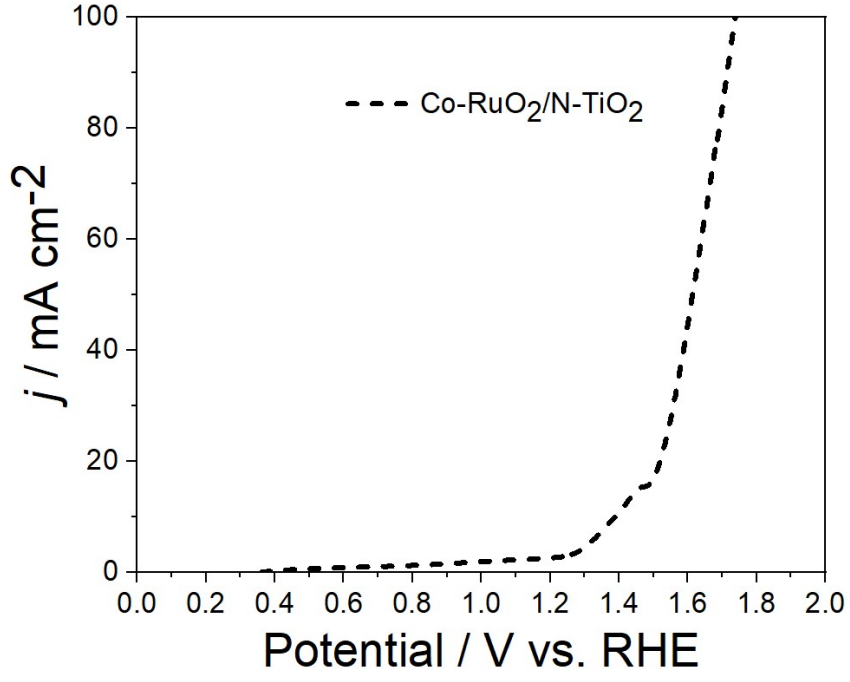

Fig. S32 Co-RuO_2/N-TiO_2 as bifunctional electrocatalyst for overall water-splitting in 0.5 M H_2SO_4.

Table S1. HER catalytic activities in alkaline condition of Co-RuO_2/N-TiO_2 and some other catalysts reported in recent literatures

Catalysts	Overpotential (mV)	Tafel Slope (mV dec^{-1})	Ref.
Co-RuO_2/N-TiO_2	16@10 mA cm^{-2}	41	In this work
a-Ru-TNTA	41@10 mA cm^{-2}	64	Nanoscale, 2023, 15, 17936-17945
F-Ru@TiO_2	12@10 mA cm^{-2}	25.24	Adv. Sci., 2024, 11, 2410881
MoO_2@Ru NT	22@10 mA cm^{-2}	29.1	Adv. Energy Mater., 2023, 13, 2301492
Ru-Mo_2C@CNT	15@10 mA cm^{-2}	26	Nat. Commun., 2021, 12, 4018
RuP_2/1.03CDs-900	100@10 mA cm^{-2}	61	ACS Sustainable Chem. Eng., 2020, 8, 3995-4002
RuNP-RuSA@CFN-800	33@10 mA cm^{-2}	37.1	Adv. Funct. Mater., 2023,33, 2213058
RuO_2-Fe_2O_3/HrGO NSs	239@10 mA cm^{-2}	97	International Journal of Hydrogen Energy, 2023, 48, 1813-1830
RuO_2/Co_3O_4/BeCu	36@10 mA cm^{-2}	/	Ionics, 2025, 31, 5995–6007
RuO_2@Ni-MWCNTs	20.2@10 mA cm^{-2}	/	Journal of Colloid and Interface Science, 2025, 679, 100-108
Ru-RuO_2/NC/NF	23@10 mA cm^{-2}	/	ChemCatChem, 2022, 14, e202201010

Table S2. HER catalytic activities in acidic condition of Co-RuO_2/N-TiO_2 and some other catalysts reported in recent literatures

Catalysts	Overpotential (mV)	Tafel Slope (mV dec^{-1})	Ref.
Co-RuO_2/N-TiO_2	50@10 mA cm^{-2}	27	In this work
Ru-TNTA	111@10 mA cm^{-2}	58	Nanoscale, 2023, 15, 17936-17945
D-RuO_2/TiO_2/TM	71@50 mA cm^{-2}	73.5	Chemical Engineering Journal, 2022, 431, 134072
8wt% RuO_2/TiO_2	150@10 mA cm^{-2}	82	DaltonTrans., 2023, 52, 3472-3481
Ru-TiO_2	150@10 mA cm^{-2}	97	J. Am. Chem. Soc., 2018, 140, 5719-5727.
Ru/TiO_2	286@10 mA cm^{-2}	90	J. Mater. Chem. A, 2021, 9, 10160-10168.
RuO_2@TiO_2/TP	143@100 mA cm^{-2}	94	Inorg. Chem. Front., 2022, 9, 6602-6607
Ru_2O/TiN/TiO_2@PNDCN	67@10 mA cm^{-2}	51	Catal. Sci. Technol., 2020, 10, 8265-8282
RuO_2@Ni-MWCNTs	70.3@10 mA cm^{-2}	/	Journal of Colloid and Interface Science, 2025, 679, 100-108

Table S3. OER catalytic activities in acidic condition of Co-RuO_2/N-TiO_2 and some other catalysts reported in recent literatures

Catalysts	Overpotential (mV)	Tafel Slope (mV dec^{-1})	Ref.
Co-RuO_2/N-TiO_2	195@10 mA cm^{-2}	77	In this work
RuO_2 x/TiO_2 x-180	243@10 mA cm^{-2}	82.8	Chem. Commun., 2025, 61, 15878–15881
RuO_2/Co_3O_4-RuCo@ NC	247@10 mA cm^{-2}	89	ACS Appl. Mater. Interfaces, 2019, 11, 47894- 47903
Fe_3O_4/RuO_2@NEU-7	450@10 mA cm^{-2}	305	Catal. Sci. Technol., 2020, 10, 8265-8282
12Ru/MnO_2	161@10 mA cm-2	29.4	Nat. Catal., 2021, 4, 1012-1023
Ru–Ni(OH) $_2$	228@10 mA cm^{-2}	55.2	Adv. Mater. 2024, 36, 2403151
Bi-RuO_2 SAAO	192@10 mA cm^{-2}	37.84	Adv. Mater., 2025, 37, 2417777
MD-RuO_2-BN	196@10 mA cm^{-2}	/	Nat. Commun., 2024, 15, 3982
FePb-RuO_2	194@10 mA cm^{-2}	61	J. Mater. Chem. A, 2025, 13, 8474–8483
RuO_2/MoO_3	167@10 mA cm^{-2}	65	Energy Environ. Sci., 2024, 17, 6755–6765
Sm–RuO_2−*x*–Ov	217@10 mA cm^{-2}	45.76	Energy Environ. Sci., 2025, 18, 4276–4287
RuO_2/D-TiO_2	180@10 mA cm^{-2}	43	ACS Catal., 2022, 12, 9437-9445.

Table S4. OER catalytic activities in alkaline condition of Co-RuO_2/N-TiO_2 and some other catalysts reported in recent literatures

Catalysts	Overpotential (mV)	Tafel Slope (mV dec^{-1})	Ref.
Co-RuO_2/N-TiO_2	269@10 mA cm^{-2}	89	In this work
c-Ru-TNTA	349@10 mA cm^{-2}	82	Nanoscale,2023,15,17936 –17945
D-RuO_2/TiO_2/TM	296@10 mA cm^{-2}	46.6	Chemical Engineering Journal, 2022, 431, 134072
RuO_2-NF	235@10 mA cm^{-2}	88	Nature Communications, 2019, 10, 1-8
Fe_3O_4/RuO_2@NEU-7	250@10 mA cm^{-2}	266	Catal. Sci. Technol., 2020, 10, 8265-8282
RuO_2-Fe_2O_3/HrGO NSs	386@10 mA cm^{-2}	67	International Journal of Hydrogen Energy, 2023, 48, 1813-1830
Ru-RuO_2/NC/NF	223@10 mA cm^{-2}	/	ChemCatChem, 2022, 14, e202201010
8-Ru-Co_3O_4/Ti	223@10 mA cm^{-2}	68.3	InfoMat., 2025, 7, e70003
Ru-RuO_2/C-300A	240@10 mA cm^{-2}	74.1	Adv. Sci., 2025, 12, 2414534
RuO_2-Ru/MoO_2@CC	231@10 mA cm^{-2}	58.3	Rare Met., 2024, 43, 5095–51045096
RuO_2:0.2Ce-LCO	135@10 mA cm^{-2}	64	Adv. Funct. Mater. 2024, 34, 2411094